Scientific Reports

https://doi.org/10.1038/s41598-026-44155-7

Article in Press

Performance evaluation of stabilized clay using sodium lignosulphonate

Received: 3 November 2025

Accepted: 10 March 2026

Published online: 14 March 2026

Cite this article as: Kumar A., Kumar P., Choudhary A.K. *et al.* Performance evaluation of stabilized clay using sodium lignosulphonate. *Sci Rep* (2026). https://doi.org/10.1038/s41598-026-44155-7

Ashutosh Kumar, Prashant Kumar, Awdhesh Kumar Choudhary & Bamidele Charles Olaiya

Performance Evaluation of Stabilized Clay using Sodium Lignosulphonate

Ashutosh Kumar[1], Prashant Kumar[2], Awdhesh Kumar Choudhary[3], Bamidele Charles Olaiya[4]*

[1]Department of Civil Engineering, Mohan Babu University, Tirupati, Andhra Pradesh, India-517102

[2]Department of Civil Engineering, Indian Institute of Technology (BHU) Varanasi, India- 221005

[3]Department of Civil Engineering, National Institute of Technology Jamshedpur, Jharkhand, India - 831014

[4]Department of Civil Engineering, School of Engineering and Applied Sciences (SEAS),
Kampala International University, Western Campus, Ishaka, Uganda

*Corresponding author: bmolaiya@kiu.ac.ug

Abstract: Rapid urbanization often demands the development of infrastructure on challenging soils, necessitating strengthening and improvement. This study explores the application of Sodium Lignosulphonate (LS), a by-product of the paper and wood pulp industry, as an eco-friendly, non-toxic stabilizer for low-plasticity clay (CL, PI ≈ 24%). Through a series of laboratory tests, including Atterberg's limit, unconfined compression strength (UCS), swell pressure, and CBR, the engineering properties of the stabilized soil were assessed. The results show that as the LS content increases, the plasticity index (PI) of the soil decreases, and the UCS value increases, reaching a maximum UCS value at 0.75% LS content. Higher LS dosages (>0.75%) resulted in gradual strength reduction due to excessive polymer chain formation and particle repulsion. Additionally, CBR tests on the soil treated with 0.75% LS after a 14-day curing period revealed significant improvements. Microstructural analysis demonstrated that LS created a bonding substance that coated soil particles, filling pores and binding them together, thereby enhancing soil stability and strength. Furthermore, increasing the curing time further

enhanced strength and reduced swelling characteristics, as LS established a strong bonding between soil particles. This research underscores the potential of LS as a soil stabilizer, offering durability and sustainability to infrastructure in urban areas facing challenging soil conditions.

Keywords: Clay; Sodium Lignosulphonate (LS); Unconfined Compression Strength (UCS); CBR; Curing period; SEM

1. Introduction

Clayey soils are characterized by their fine particle size and high-water retention, which present challenges in various construction projects. Their tendency to undergo volumetric changes in response to variations in moisture often leads to foundation failures and structural instability. The stabilization of clayey soil is a technique that aims to improve its properties and enhance its suitability for construction purposes. In the past, researchers[1,2] have developed numerous methods to mitigate the impact of clayey soil on the infrastructure constructed upon it. Chemical stabilization using cement, lime, and fly ash is common, but these traditional admixtures raise serious environmental concerns. For example, Portland cement production releases approx. 0.8-1.0 t CO_2 per tonne of cement[3], while lime stabilization significantly increases soil pH (typically >12), causing corrosion of buried infrastructure and long-term alkalinity issues[4]. Traditional admixtures enhance the workability of expansive soils while reducing their potential for expansion. However, the use of these alkaline stabilizers may raise environmental and workplace health and safety concerns. Underground gas lines, power lines, and pipes may corrode and deteriorate[5-12], posing serious environmental problems such as increased soil alkalinity[13-15] and higher greenhouse gas emissions during their production[16-17]. Therefore, there is a need for alternative stabilizing agents, such as waste by-products and bio-based products[18-20].

To address these issues, lignosulfonate (LS), a by-product of the paper and timber industry, has emerged as a promising eco-friendly stabilizer[21-25]. Sodium lignosulphonate (LS) is an anionic polyelectrolyte containing sulphonate groups (SO_3^-), which confer high water solubility and strong negative surface charge compared to unmodified lignin. These sulphonate

groups enhance electrostatic interaction and cation-exchange capacity with clay surfaces, distinguishing LS from non-sulphonated lignin derivatives[26-28]. Lignin is an abundant and renewable biopolymer, and its application as a soil stabilizer aligns closely with global sustainable development and circular economy objectives[29–31]. In recent years, increasing emphasis has been placed on the valorization of bio-based and agricultural residues in construction materials as environmentally responsible alternatives to conventional binders, a trend that has been widely documented across cementitious and composite-based applications[32,33]. Within geotechnical engineering, numerous studies have reported the effectiveness of lignin used alone or in combination with chemical additives for soil stabilization. For example, stabilization of clayey soils and silty sands using sodium dichromate–lignin mixtures was shown to significantly enhance strength and durability[34]. Similarly, Sharmila et al.[35] demonstrated that lignin effectively reduces swell potential in expansive soils, thereby improving dimensional stability.

Unlike traditional stabilizers such as Portland cement or lime, lignin-based by-products exhibit complex physicochemical characteristics that vary considerably depending on source material, processing method, and chemical composition. Comparable variability has also been reported for other agricultural and industrial waste-derived construction materials, where performance is strongly influenced by raw material origin and treatment conditions[32,36]. This inherent variability underscores the need for material-specific investigations when adopting bio-based stabilizers in geotechnical applications.

Most previous studies on lignosulphonate (LS)-treated soils have focused on high-plasticity clay (CH), silty clay, and sandy silt[20, 37–43], while low-plasticity clay (CL) has received comparatively limited attention. Although CL soils generally exhibit lower swell–shrink potential than CH soils, they frequently pose significant engineering challenges in practice. These include low undrained shear strength (typically 50–150 kPa), high compressibility, reduced bearing capacity under saturated conditions, and susceptibility to strength degradation and rutting under repeated traffic

loading. Such deficiencies often render untreated CL soils unsuitable for direct use as subgrade or foundation materials in roads, embankments, and lightly loaded structures, particularly in regions subjected to seasonal moisture variations.

From a sustainability perspective, even modest improvements in the strength and stiffness of CL soils through stabilization can yield substantial benefits, including reduced pavement thickness, lower material consumption, and decreased construction costs. This approach is consistent with broader sustainable construction strategies that emphasize resource efficiency, waste utilization, and life-cycle performance optimization[44-46]. However, despite the growing interest in bio-based stabilizers, limited research has specifically examined the geotechnical behavior of sodium lignosulphonate-treated low-plasticity clay (CL). This knowledge gap highlights the need for targeted experimental investigations to evaluate the suitability, performance mechanisms, and engineering implications of lignin-based stabilization for CL soils. Furthermore, the study examines the linkage between macroscopic engineering improvements and underlying microstructural evolution through scanning electron microscopy (SEM) and energy-dispersive X-ray spectroscopy (EDS). Particular attention is given to expected changes such as particle flocculation and aggregation induced by electrostatic interactions, physical coating and bridging of clay particles by lignosulphonate polymer chains, pore-space reduction and densification of the soil matrix, and formation of stable soil-lignosulphonate bonds. These microstructural alterations are anticipated to directly account for the observed gains in strength, stiffness, and resistance to swelling at the macroscopic level. In view of this, the primary aim of the present study is to investigate the effect of various LS content on the strength and deformation characteristic of stabilized low plastic clay using laboratory tests (i.e., Atterberg limits, unconfined compressive strength (UCS), CBR, and swelling pressure tests). The results of this study were also evaluated using scanning electron microscope (SEM) analysis

by observing the micro-structural changes of the soil before and after the stabilization.

2. Experimental investigation

2.1 Materials

2.1.1 Clay (CL)

The soil was taken at a depth of roughly 3 meters from the backyard of NIT Jamshedpur, near the Kharkai River in Jharkhand, India. Basic soil properties are presented in Table 1, and Figure 1 illustrates the soil gradation based on ASTM D6913[47]. The Atterberg limits test, conducted following ASTM D4318[48], revealed liquid and plastic limits of 49.85% and 25.77%, respectively, resulting in a plasticity index (PI) of approximately 24%. According to the ASTM D2487[49], this soil is classified as low plastic clay. Compaction tests, performed according to ASTM D698[50], indicated an optimum moisture content of 20.23% and a maximum dry weight of 16.67 kN/m^3 for the clay. Soil pH was determined using a Portable pH meter, following ASTM D4972[51]. The soil primarily consists of silt-sized particles (53%) and approximately 32% clay-sized particles. Additionally, the specific gravity was 2.71, as per ASTM D854[52].

Table 1. Engineering Properties of Soil Investigated

Laboratory test	Value
Specific gravity (G)	2.71
Liquid Limit (LL) %	49.85
Plastic Limit (PL) %	25.77
Plasticity Index (PI) %	24.08
IS Soil Classification	Medium Plasticity Clay (CI)
OMC %	20.23
MDD, γ_{dmax} (g/cc)	16.67 kN/m^3
pH	7.9
UCS (at OMC)	241 kPa
Free Swell Index (FSI) %	47

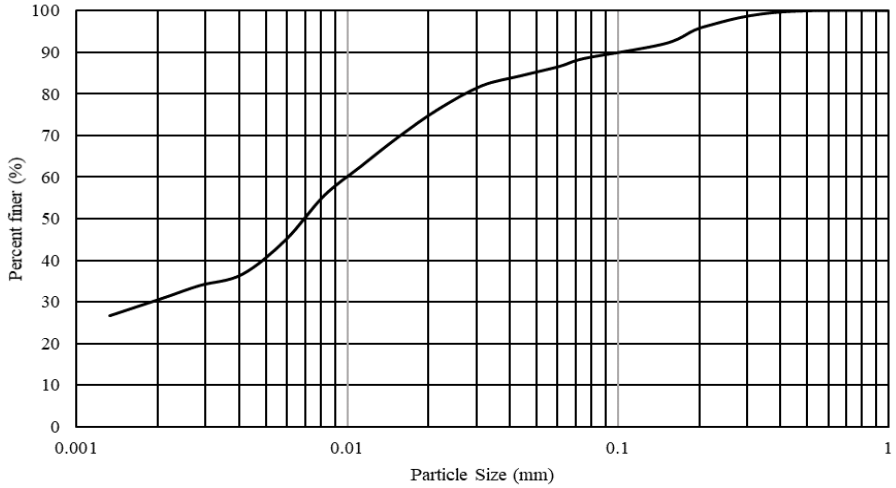

Fig. 1 Particle size distribution

2.1.2. Sodium Lignosulfonate (LS)

Sodium Lignosulfonate is an organic polymer molecule derived as a byproduct of paper, wood, and biomass processing. Traditionally, LS has been regarded as a waste product or a low-value industrial by-product in both industrialized and developing countries. The worldwide paper and biomass industries generate substantial quantities of lignin-based by-products after extracting essential fiber or wood pulp. LS typically exists in the form of a solid powder or a dark liquid with high moisture content. The LS utilized in this test, as illustrated in Figure 2, is a dark-brown powder that is water soluble.

(a) (b)

(c) (d)

(e)

Fig. 2. Sample preparation for UCS Test (a) Clay (b) Sodium Lignosulphonate (LS) (c) Clay + LS + water (d) UCS Sample (e) Curing of UCS sample

2.2 Laboratory test

The laboratory tests include Atterberg limits, unconfined compressive strength (UCS), CBR, and swelling pressure tests were conducted on the stabilized specimens with various LS dosages. For our study, the maximum dry unit weight and optimum moisture content of the virgin soil were used for preparing the treated specimens. Scanning electron microscope (SEM) and Energy-dispersive X-ray spectroscopy (EDS) analysis were used to understand the microstructural changes to interpret the results. LS, chosen as a stabilizer in percentages of 0.5%, 0.75%, 1%, 2%, 3%, and 4% by the dry weight of the soil[15, 22].

2.2.1. Atterberg limits tests

Atterberg limits test performed according to ASTM D 4318[48], the specified amount of LS and water (approximately equal to the Optimum Moisture Content) were thoroughly mixed with air-dried soil. This mixture was then sealed in a double plastic bag and placed in a controlled temperature environment (a desiccator) for 24 hours before conducting the Atterberg limit test.

2.2.2. Unconfined compression strength (UCS) test

The UCS test was performed according to ASTM D 2166[53], determining the soil's shear strength using cylindrical specimens at a fixed strain rate of 1% per minute. Furthermore, an analysis was conducted to determine how admixture affected the shear strength of the treated soil. To prepare the treated specimens, different doses of LS (0%, 0.5%, 0.75%, 1%, 2%, 3%, and 4% by dry soil mass) were mixed with water as per[54]. The LS-water mixture was then combined with oven-dried soil, whose weight had been previously determined. This mixture was thoroughly mixed to achieve a homogeneous mixture. The homogeneous soil mixture was uniformly compacted in a Proctor mould to obtain specimens of the required size (50 mm × 100 mm). These compacted specimens were wrapped in plastic, sealed in double plastic bags, and placed in a desiccator in a temperature-controlled environment for varying curing durations (0 days, 7 days, 14 days, and 28 days) as shown in Figure 2.

2.2.3. pH test

The effect of the lignin stabiliser on soil pH was evaluated with an Eutech pH meter[51] pH tests were conducted on treated samples with the optimum content of Sodium Lignosulfonate obtained from the UCS test. A measuring beaker was filled with approximately 10 g of air-dried soil and 10 mL of deionized water (liquid to solid ratio is 1.0). After stirring for a few seconds, the solution was allowed to stand for an hour. Subsequently, the soil-water mixture was tested for pH, with the pH probe positioned in the beaker, and the readings were averaged.

2.2.4. California Bearing Ratio (CBR) test

The CBR test was performed according to ASTM D 1883–14[55], which determined the soil's CBR value. The CBR value was calculated as the ratio of the applied load required to penetrate a standard well-graded crushed stone material to the unit force needed for 2.5 or 5 mm of penetration. CBR tests were conducted on treated samples with the optimum content of sodium lignosulfonate, as determined by the UCS test. CBR test samples were poured into a steel mould, and these samples were wrapped in plastic and then placed in a temperature-controlled environment (desiccators) for curing.

2.2.5. Swell pressure test

The swell pressure test was conducted following ASTM D 4546[56] to determine the amount of vertical free swell strains. Swell pressure tests were conducted on treated samples with the optimum content of sodium lignosulfonate, as determined by UCS and CBR tests. To prepare the treated specimens, optimum content of LS was mixed with water. The LS-water mixture was then combined with oven-dried soil, and the mixture was thoroughly mixed to achieve homogeneity. The swell test samples were compacted into consolidometer rings (50 mm in diameter and 20 mm in height) after cutting suitable-sized samples from the material obtained from the standard Proctor mould. These compacted specimens were wrapped in plastic, sealed in double plastic bags, and placed in a desiccator in a temperature-controlled environment for varying curing durations (0 days, 7 days, and 14 days).

2.2.6. Microstructure Analysis

Microstructure images of the unstabilized and stabilized samples were obtained to gain a better understanding of the results. Based on SEM and EDS analysis, the stabilization mechanisms of treated specimens discussed and the observations from the tests were explained.

3. Result and discussion

3.1 Atterberg Limits Tests

The liquid limit and plasticity index of the untreated soil are found to be 49.85% and 25.77%, respectively. The variation in liquid limit (LL) and plasticity index (PI) of both the virgin and lignin-stabilized soil is shown in Figure 3. Both LL and PI of the lignin-stabilized soil were slightly lower than those of the untreated soil. The addition of lignin reduced LL by 15% and PI by 28.3% at a lignin content of 0.75%. However, plastic limit (PL) of the lignin-stabilized soil remained almost the same as that of the untreated soil, as shown in Table 2. From the Table 2, the initial reduction in LL and PI up to 0.75% LS is attributed to edge-to-face flocculation caused by adsorption of negatively charged sulphonate groups onto positively charged clay edges, which increases effective particle size and reduces the thickness of the diffuse double layer. However, beyond 0.75% LS, excess anionic polymer molecules accumulate in the pore fluid and on the negatively charged basal surfaces of clay platelets. This introduces additional negative charges that thicken the diffuse double layer again and generate strong inter-particle repulsion, leading to a more dispersed fabric and a consequent rise in LL and PI. This reversal is directly confirmed by scanning electron microscopy (SEM) whereas the optimum 0.75% LS specimen exhibits dense, aggregated clusters (Fig. 14).

Table 2. Atterberg limit results of treated clayey soil

Soil nature	Admixture content (%)	Liquid limit (LL) (%)	Plastic limit (PL) (%)	Plasticity index (PI) (%)
Virgin soil	0	49.85	24.08	25.77
Lignin-treated soils	0.5	46.3	23.93	22.37
	0.75	42.3	23.84	18.46
	1	43.1	23.97	19.13

2	44.6	24.1	20.5
3	45.9	24.14	21.76

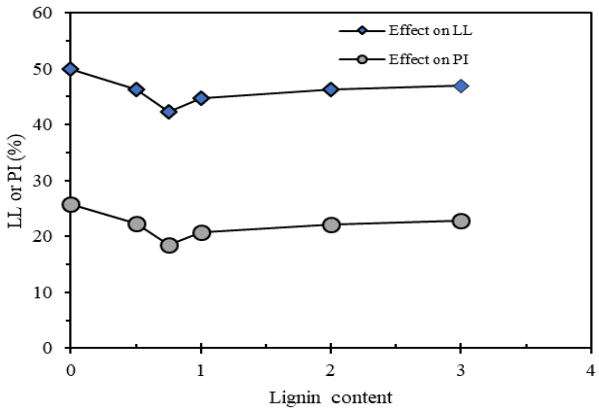

Fig. 3 Lignin content effect on Atterberg limits

Besides, this can be observed on the plasticity chart, as shown in Figure 4, where both lignin-treated and untreated soils fall within the CI zone. However, the position of the 0.75% lignin-treated soil is very close to the A-line, indicating a reduction in the diffuse double layer (DDL) thickness due to floc formation by the soil particles and lignin. As the lignin content increases, the soil molecules expand due to the excessive formation of lignin chains carrying a negative charge.

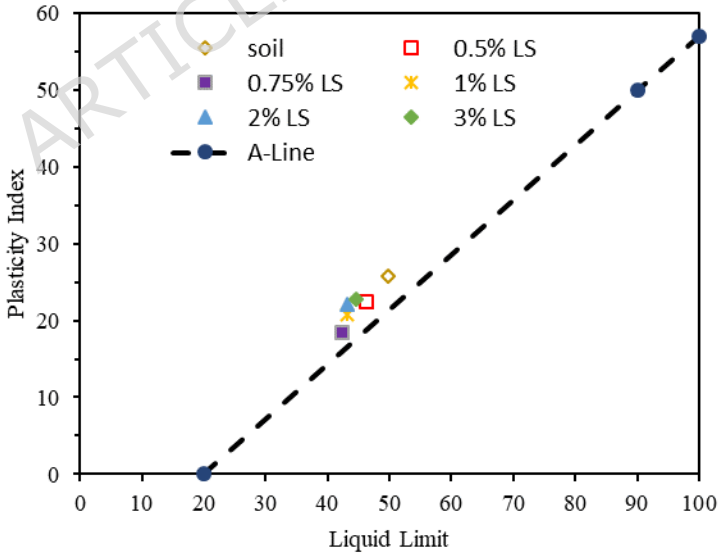

Fig. 4 Plasticity index-based classification of lignin-treated soil

3.2 Unconfined Compressive Strength (UCS) Test

Further UCS tests were conducted to assess the strength properties of the lignin-treated soil after 0, 7, 14, and 28 days of curing. Figures 5(a-f) depict

the variations in UCS test values with different lignin contents at various curing periods. It is observed that as the curing time increases, the UCS value improves. For example, Figure 5(a) shows that with a lignin content of 0.5%, the UCS value increases from 236 to 345 kPa with increase in curing period from 0 to 28 days, representing an approximate 46% increase in strength. Figure 5(f) indicates that with a lignin content of 4%, there is a 33% increase in strength after a 28-day curing period. This suggests that increasing the curing period, the strength of the stabilized clayey soil increases significantly with increasing additive content when compared to the natural clay.

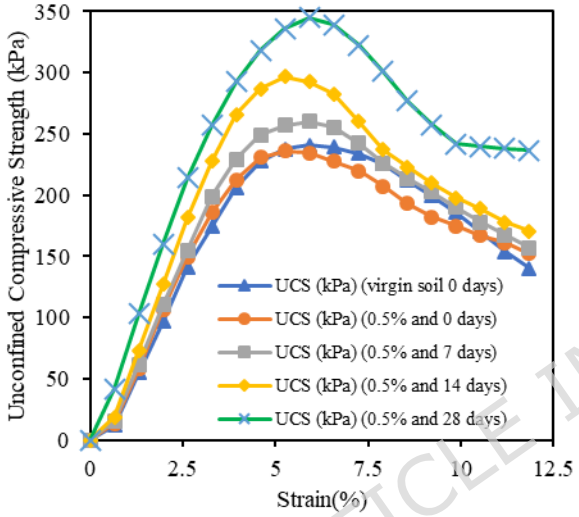

(a) 0.5% lignin treated clay

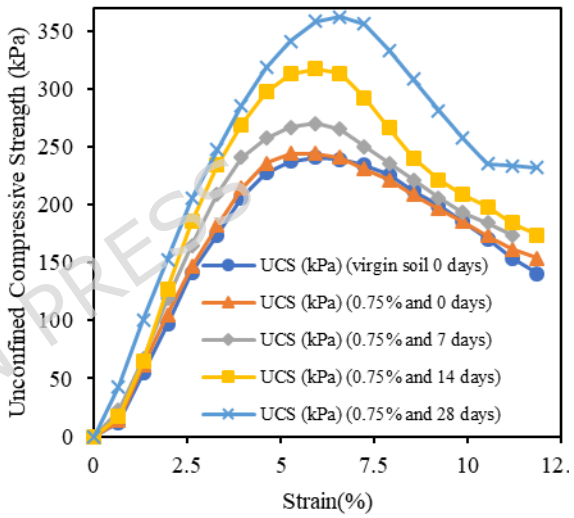

(b) 0.75% lignin treated clay

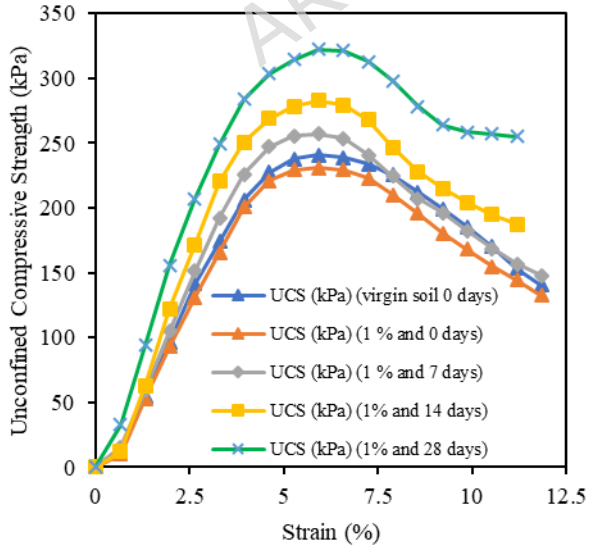

(c) 1% lignin treated clay

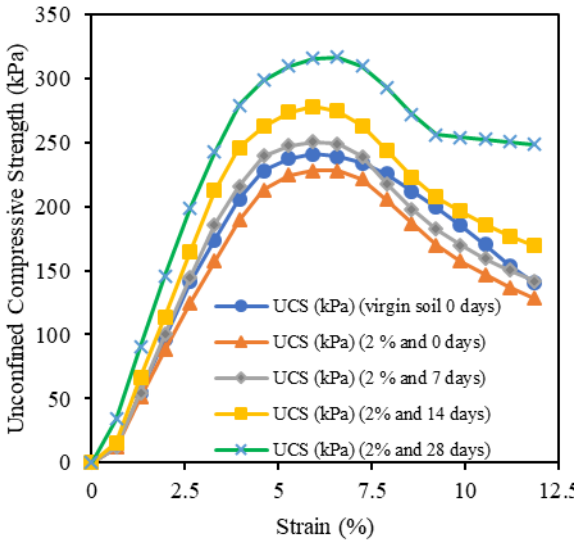

(c) 2% lignin treated clay

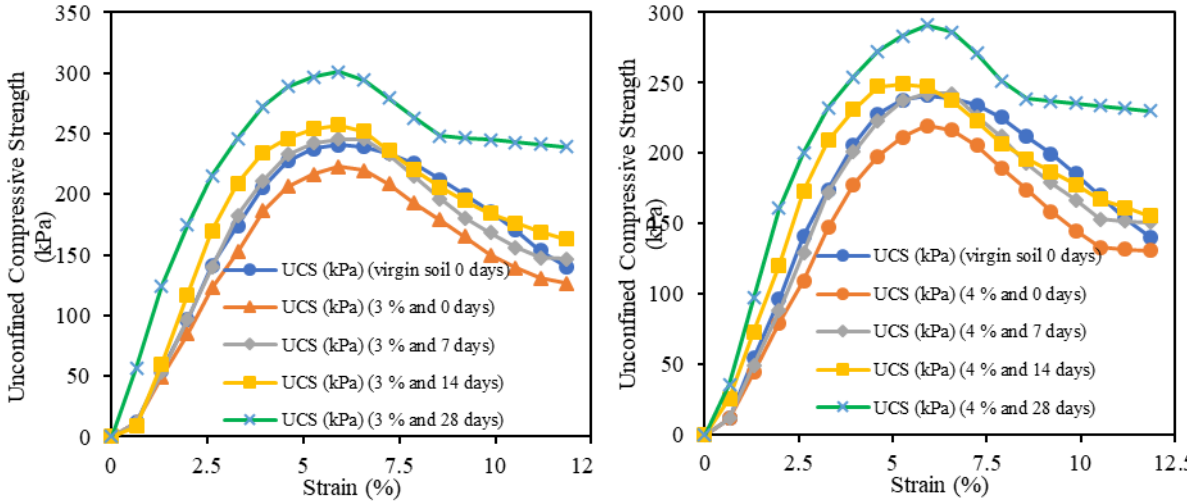

(e) 3% lignin treated clay (c) 4% lignin treated clay

Fig. 5 Stress-strain curves at 0, 7, 14, and 28 days of curing at different lignin content

Figure 6 illustrates the influence of lignin concentration on UCS magnitude during 28-day curing periods. The UCS value of the virgin soil is included in the graph for comparison. The UCS value progressively increases as the lignin concentration rises from 0% to 0.75%. Table 3 reveals that after curing for 28 days, the UCS value of the 0.75% lignin-treated soil increases from 241 to 362 kPa, representing a 50% increment. However, with further increases in lignin content, this value decreases. The decrease in UCS beyond 0.75% LS is attributed to excessive negatively charged lignosulphonate polymer chains that are no longer fully adsorbed onto clay particles. These surplus anionic chains increase inter-particle repulsion and prevent the close packing and effective bonding achieved at the optimum dosage. Direct microstructural evidence supporting this mechanism is provided by scanning electron microscopy, specimens treated with 3% and 4% LS exhibit a markedly looser and more dispersed fabric compared to the dense, flocculated aggregates observed at 0.75% LS. This behaviour is in excellent agreement with previous studies on lignosulphonate and other anionic polymer stabilizers. Ta'negonbadi and Noorzad[28] reported similar strength reduction beyond optimum dosage due to repulsion between excess negatively charged molecules. Alazigha et al.[29] and Indraratna et al.[22] also observed that excessive lignosulphonate

leads to particle dispersion and loss of inter-particle bonding. Therefore, 0.75% lignin is deemed optimal for this clay. This unusual behaviour results from a decrease in stress values as lignin concentration increases further. It is primarily due to the excessive formation of lignin polymer chains compared to the clay binder, possibly leading to repulsion between these charged particles. Moreover, when moisture content is kept constant, increasing lignin concentration reduces the compressibility of the mixture, indicating opposing attractive forces that result in a decrease in UCS value.

Table 3. Effect on UCS with curing time

Curing Period	0.5% lignin	0.75% lignin	1 % lignin	2 % lignin	3 % lignin	4 % lignin
0 days	236	244	231	228	223	219
7 days	260	270	257	250	245.6	242
14 days	297	317	283	271	257	249
28 days	345	362	322	316	301	291

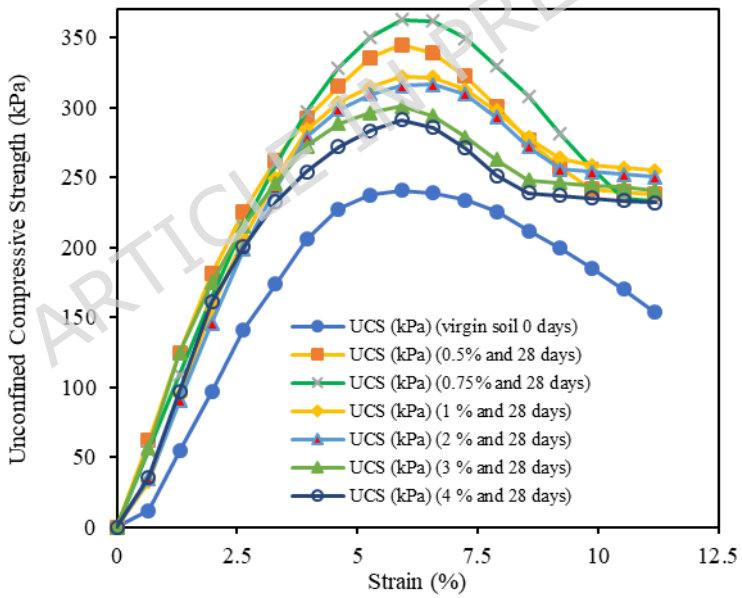

Fig. 6 Stress-strain curves of 28 days cured lignin-treated clay

Figure 7 shows that at the early stages (0 days), nearly all lignin-treated soils had lower UCS than untreated soils, which was expected due to lower cluster development. However, at longer curing durations (7, 14, and 28 days), soils treated with lignin exhibited higher UCS values. This increase in UCS can be attributed to the neutralization of negative electrical charges on the clay surface and a reduction in the size of clay minerals'

crystals, allowing stable aggregations to form. As seen in Figure 6, increasing the curing period positively influences UCS in lignin-treated soils. Therefore, stabilization may depend on curing, as there is adsorption, coating, and agglomeration of soil particles under laboratory conditions, which is time-dependent.

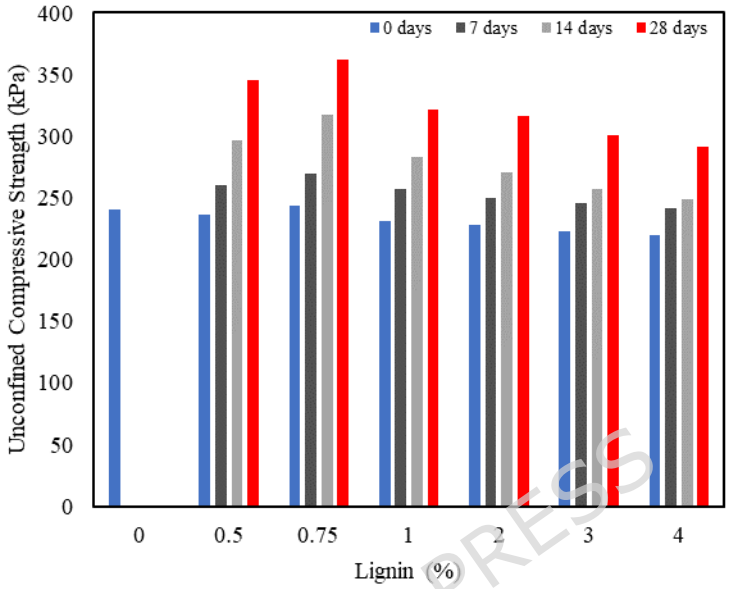

Fig. 7 Influence on the UCS at various lignin content

3.3 pH Test

After obtaining the UCS test results, a pH test was performed. Figure 8 illustrates the variations in the pH of the soil stabilized with lignin after 28 days of curing. The mean pH results for the untreated soil and the samples treated with 0.5%, 0.75%, 1%, 2%, 3% and 4% lignin are found to be 7.9, 8.28, 8.36, 8.38, 8.46, 8.51, and 8.63, respectively. It is evident from Figure 7 that the pH values of the stabilized soil increase with higher percentages of lignin, although the increase is minimal. After 28 days, the pH changes at different lignin content levels are all below 0.4. This slight change in pH could be attributed to the minimal quantity of lignin required for soil stabilization or to complex chemical processes between lignin and clay particles that alter the pH of the stabilized clay. pH levels can potentially impact plants, fauna, and subsurface water. These results are valuable for defining environmentally acceptable soil additives for stabilizing unstable clayey soils using organic industrial by-products.

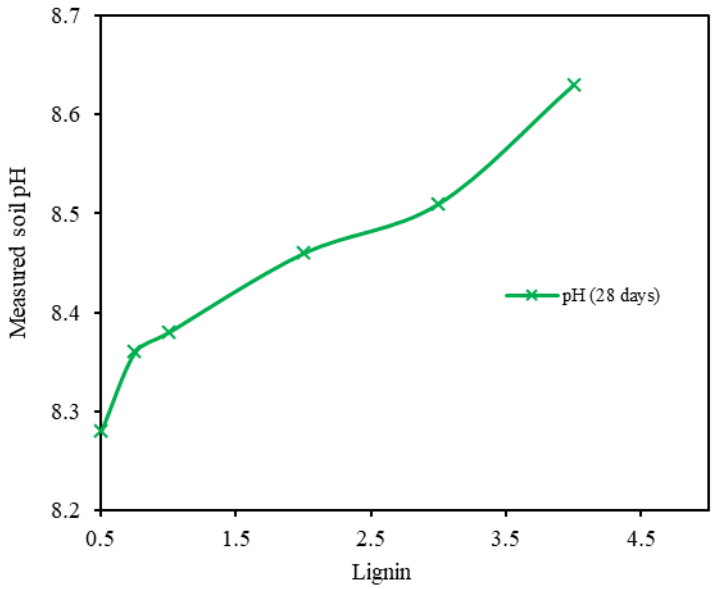

Fig. 8 pH variation of 28 days cure lignin-treated clay

3.4 California Bearing Ratio (CBR) Test

The graphical relationship between load intensity and penetration of the stabilized specimens is depicted in Figure 9. It shows that the soil's bearing capacity increases with an optimum lignin content of 0.75%. Initially, the variations in curing time for lignin-treated soil are not significant. However, it becomes evident that with increasing curing time, higher load-intensity values are obtained for the same penetration. Figure 10 represent the variations in CBR test results with the optimum lignin percentage (0.75%) at different curing times (1 day, 7 days, and 14 days). Here, the 1-day CBR represents the immediate bearing capacity after compaction, which is relevant for early construction stages. The 7- and 14-day tests were selected to capture early-age strength development due to hydration and bonding reactions in the stabilized soil. These curing periods are commonly used to evaluate short-term performance prior to longer-term strength gain. From the Figure 10, it is observed that compared to untreated soil, the CBR% of lignin-stabilized soil is significantly higher. Additionally, as the curing period increases, the CBR% continuously rises. After 14 days of curing, there is approximately a 30% increase in the CBR value. This indicates that particle surfaces in the soil adsorbed a thin layer of lignin, expelling water from the matrix. Consequently, the stabilized soil

can be compacted more densely. This observation may be attributed to the adhesive material produced during stabilization, which binds the soil particles together by coating them, resulting in a stronger soil structure.

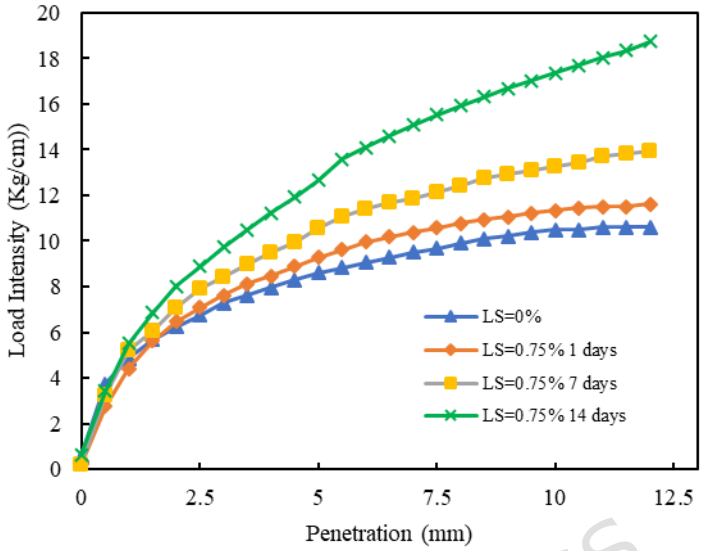

Fig. 9 Load Intensity-penetration curves of lignin-treated clay

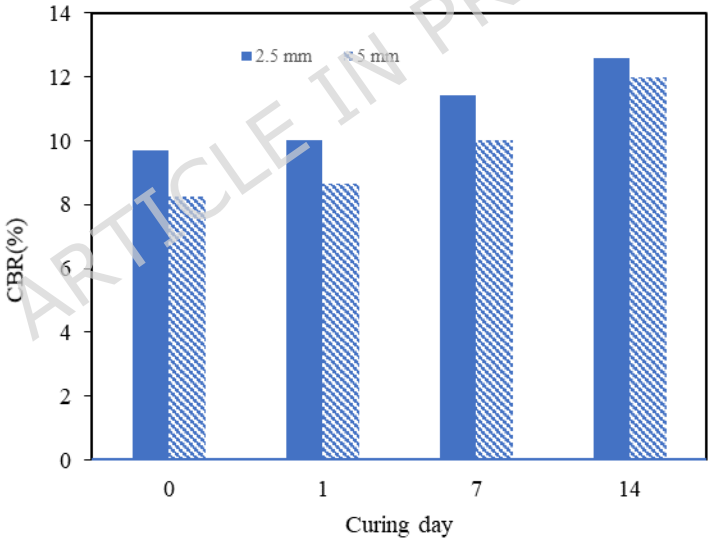

Fig. 10 Effect on CBR at different curing period

3.5 Swell Pressure Test

Swell pressure tests were conducted to understand the swelling phenomenon of both the virgin soil and the 0.75% lignin-treated soil. Figure 11 illustrates the impact of lignin content on swell potential over time. With 0.75% lignin treatment, the percentage swelling reduced from

4% to about 3.2%, indicating a decrease in soil swelling behaviour. This 20% reduction in swelling potential signifies a significant decrease in swelling. Additionally, the soil's plasticity index decreased after lignin treatment, indicating reduced soil wettability and, consequently, a decrease in soil swelling.

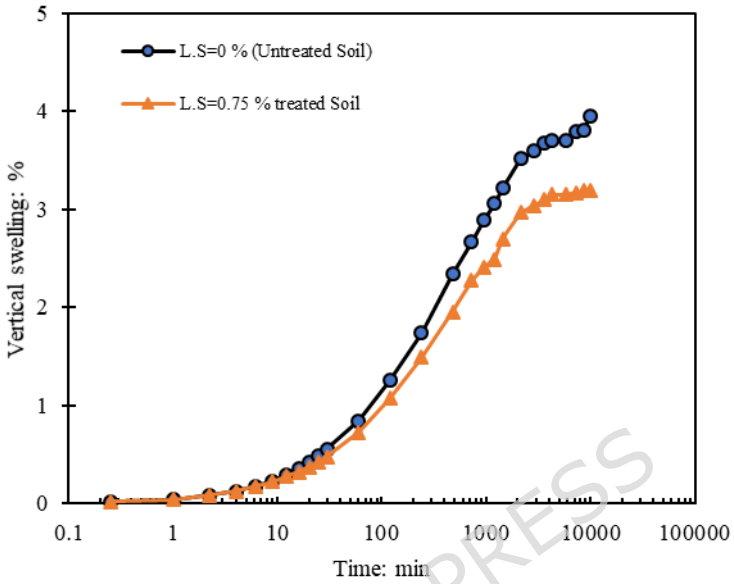

Fig. 11 Vertical swelling vs time response

After completing the swell potential test, swell pressure measurements were conducted on both the virgin and lignin-treated soil as shown in Figure 12. It was found that the soil had a swell pressure value of 185 kPa, which reduced to 165 kPa in the lignin-treated soil due to its limiting effect on swelling. Under a surcharge of 200 kPa, the treated soil sample exhibited more compression compared to the virgin soil. This observation may be explained by the natural characteristics of the virgin soil, which tends to swell more than the treated soil under the same surcharge pressure. The reason for this behaviour may be attributed to the nature of the admixture, as polymeric admixtures typically contain both hydrophobic and hydrophilic groups. The hydrophobic element enhances chemical bonding on clay particle surfaces, preventing water from adhering to them and reducing the soil's tendency to swell.

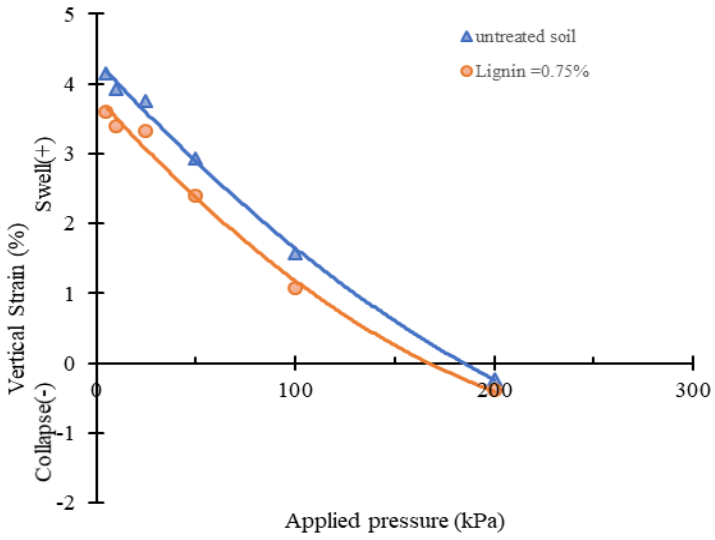

Fig. 12 Swelling pressure measurement of soil

3.6 Scanning Electron Microscope (SEM) Analysis

The SEM was used to capture digital images of soil structures for qualitative analysis of the lignin stabilization process. As shown in Figure 13, untreated clayey soil particles are clearly separated from each other and lack a distinct cementing characteristic. At a 10 µm magnification, SEM images of untreated expansive soil reveal clay particles with inter- and intra-aggregate pores forming a clay aggregate structure. SEM micrographs of 0.75% lignin-treated soil samples after a 28-day curing period are presented in Figure 14(a) and (b), illustrating the agglomeration of soil particles with larger voids and somewhat larger-sized particles. When lignin is introduced to the soil, it covers and binds the soil particles with a cementing substance thereby significantly reducing the soil's pore volume.

Vinod et al.[21] suggest that the reactive functional groups of recycled lignin and clay minerals undergo a cation-exchange process, potentially responsible for the flocculated state of the fabric. This effective development of lignin-based cementing materials leads to the filling of large pores and enhances the cementation bonding of soil aggregates, resulting in the formation of a robust microstructure in stabilized soil.

Based on the SEM images, it can be concluded that lignin serves as a binding agent, improving the cohesion of soil particles over time. This results in the accumulation of larger aggregates, leading to a strong soil

structure capable of withstanding applied loads. This improvement is reflected in parameters such as shear strength and UCS values. The micrographs show that the addition of lignin to treated soil induces flocculation and aggregation, creating a stable structure with coarser particles and a strong bond that enhances resistance to applied shear and compressive stresses. This, in turn, increases the strength properties of treated soils. Therefore, microstructural analysis enhances our understanding of the test findings related to stabilized soils. It should be noted that SEM observations (e.g., improved matrix densification and reduced visible voids) are presented only as supporting visual trends. The primary evidence for performance enhancement remains the experimentally measured mechanical properties.

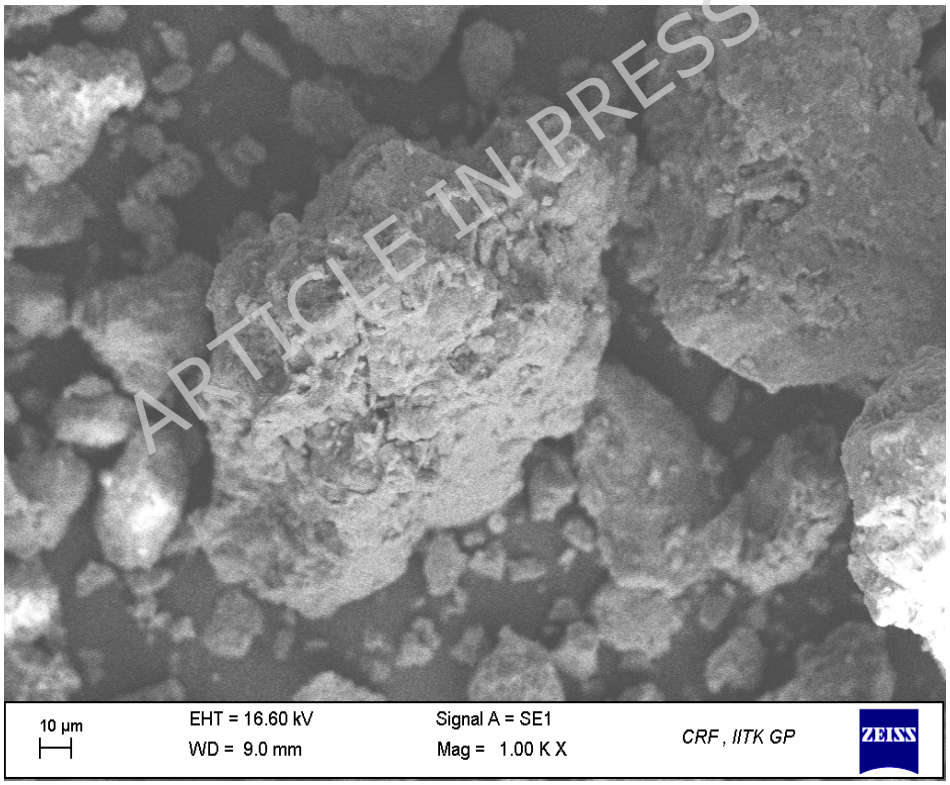

Fig. 13 SEM images of untreated soil

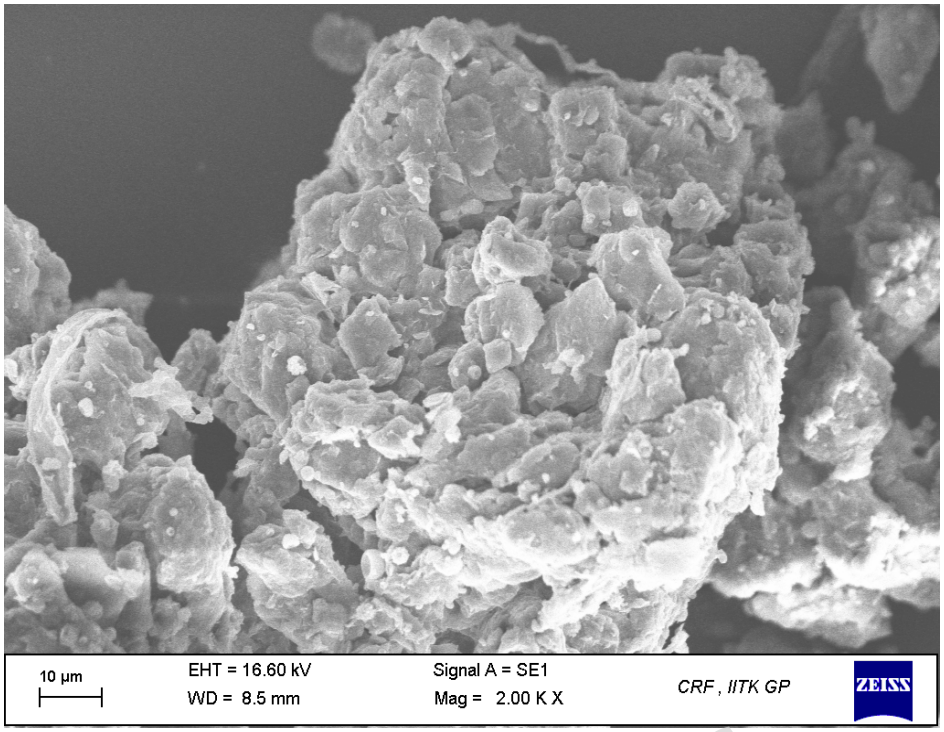

(a)

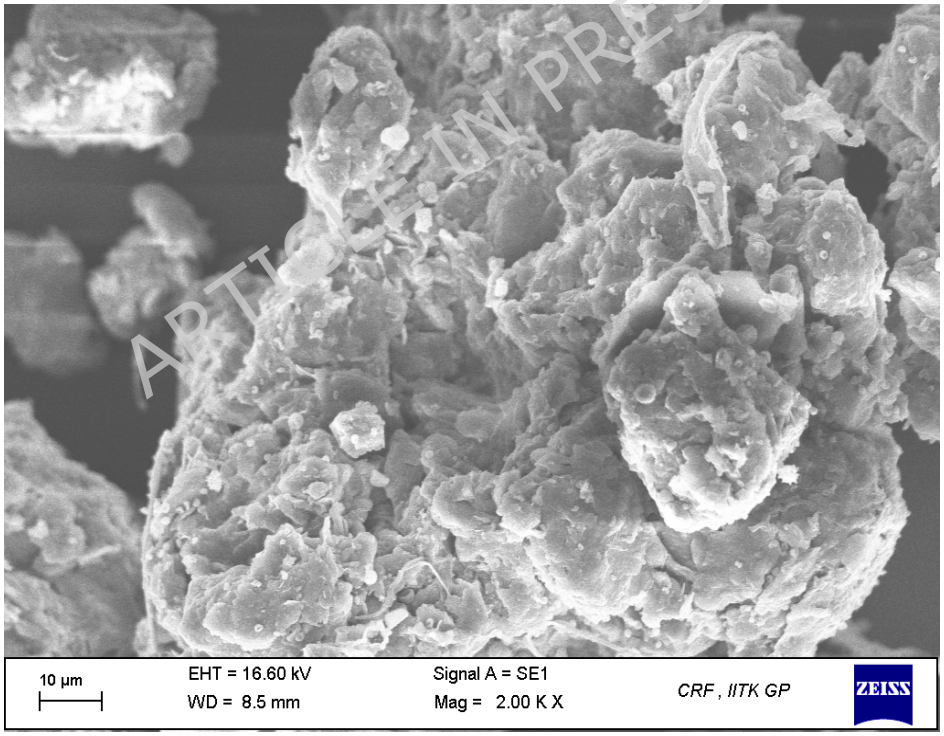

(b)

Fig. 14 SEM images of 0.75% lignin stabilized soil

3.7 Energy-dispersive X-ray spectroscopy (EDS) analysis

Figure 15 and Figure 16, depicting images of virgin and lignin-stabilized soil, show minimal intensity changes between the wavelengths of the two

sample sets. This suggests that there was no significant chemical reaction between the sorbate (lignin mix) and the absorbent (soil minerals). Table 4 provides a quantitative assessment of the elements in each soil sample. Following lignin treatment, only slight changes in elemental ratios occurred; for instance, the Aluminium (Al): Silica (Si) ratio changed by approximately 14 percent. Aluminium and silica were chosen for analysis as they are components of clay minerals, and a decrease in the aluminium-silica ratio could indicate a structural alteration in the tetrahedral sheets due to the exchange of octahedral Al^{3+} cations with the admixture. Silica release from clay minerals, similar to natural soil weathering, can occur when the Al:Si ratio increases. In the untreated soil, aluminium and silica levels were 7.56g and 22.22g, respectively. After treatment, these levels remained nearly the same (7.82g for aluminium and 19.73g for silica). The Al:Si ratio increased slightly from 0.3402 to 0.3963 after treatment, indicating a modest variation in soil mineralogy (Table 4). It is important to note that specimen topography may influence Al:Si study data, cautioning against drawing strong conclusions.

Table 4. Soil element content before and after EDS treatment

Element	**Weight (%) Lignin = 0%**	**Weight (%) Lignin = 0.75%**	**Al:Si of Virgin soil**	**Al:Si of treated soil**	**% change Al:Si**
C	19.07	23.19			
O	40.63	36.41			
Na	1.35	0.93			
Mg	0.51	0	0.3402%	0.3963%	14.1%
Al	7.56	7.82			
Si	22.22	19.73			
Fe	8.66	10.33			
Ca	0	1.59			
Totals	100	100			

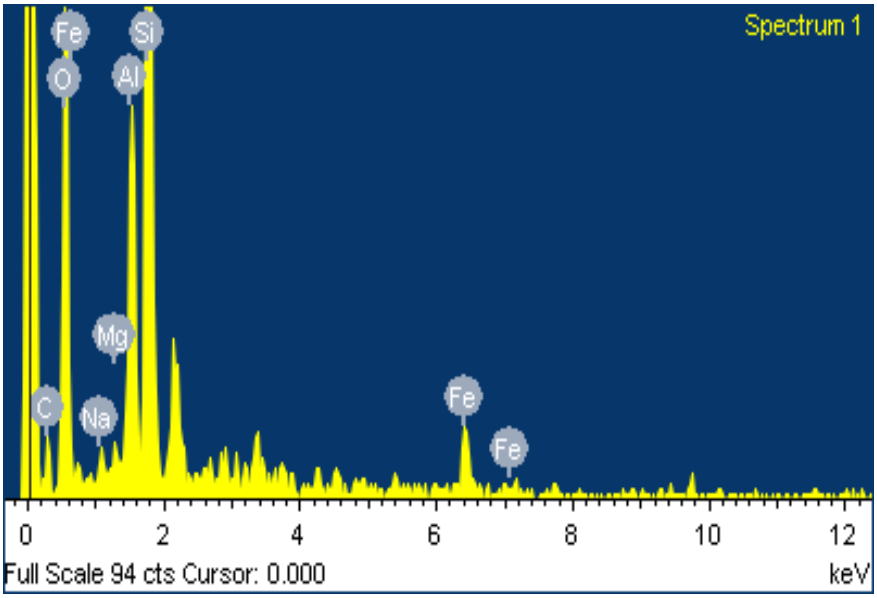

Fig. 15 EDS frequency of virgin soil

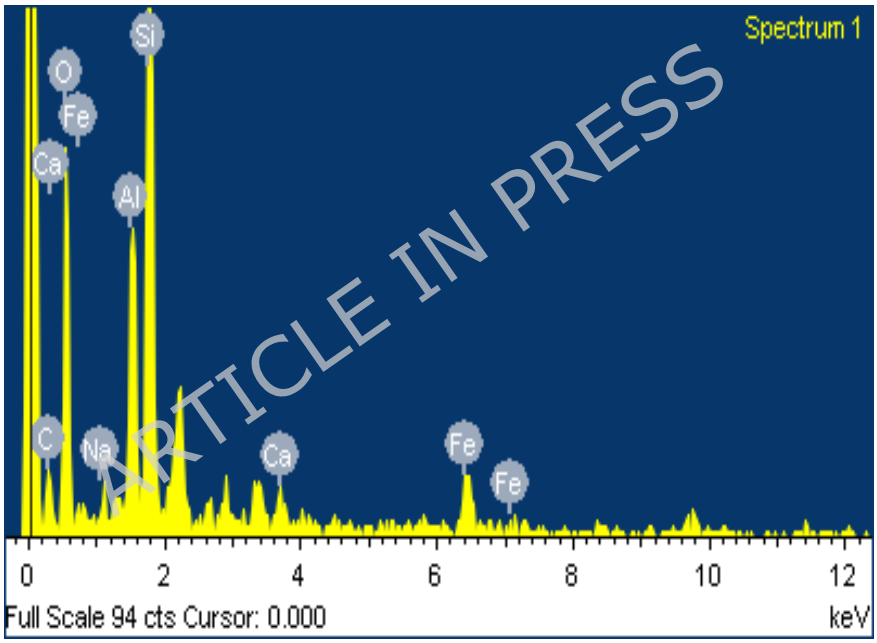

Fig. 16 EDS frequency of 0.75% lignin stabilized soil

3.8 Mechanism

The interaction mechanism between soil and lignin significantly affects the mechanical performance of lignin-treated soil, particularly in enhancing its strength and swelling properties. This interaction mechanism differs significantly from that of traditional admixtures. Therefore, this research investigates this mechanism based on test data and proposes a possible mechanism for lignin-stabilized soil. The addition of 0.75% lignin reduced the soil's liquid limit by 7%, indicating a decrease in double-layer thickness

and suggesting an electrostatic reaction between soil and lignin, potentially reducing the negative charge of clay particles. However, Lignosulphonate (LS) primarily acts as a flocculating and binding agent rather than a cementing agent like lime or cement. The strength gain is mainly attributed to electric neutralization of clay negative charges, physical coating and bridging of particles by anionic polymers chains. Besides, Strength tests also demonstrated that soil treated with 0.75% lignin and allowed to cure for 28 days exhibited an improved unconfined compressive strength of 362 kPa. This increase in strength may be attributed to lignin's cementing and bonding properties, which bind clay particles together, consolidate them, and enhance strength. Various factors, including changes in pore fluid characteristics, cation-exchange processes, adsorption on clay surfaces reducing double-layer thickness, and coating on clay particles, contribute to this aggregating effect.

Figure 17 provides a schematic diagram of the lignin stabilization process. The reduced double-layer thickness occurs because the net positive charge of lignin neutralizes the negative charges on the clay particles. In Figure 17(a), a typical soil mineral structure can be seen where clay minerals with excess negative charges (dash) are connected by intermediate bonding materials (circle). Figure 17(b) illustrates that the addition of lignin to the soil results in electrostatic attraction, causing lignin to adsorb onto the clay mineral surface. Figure 17(c) shows that over time, lignin gradually neutralizes the excess negative charges on the clay mineral surface, leading to the development of bonds with clay particles. Ultimately, the clay particles are drawn together into aggregates or grain clusters by the lignin polymer chain.

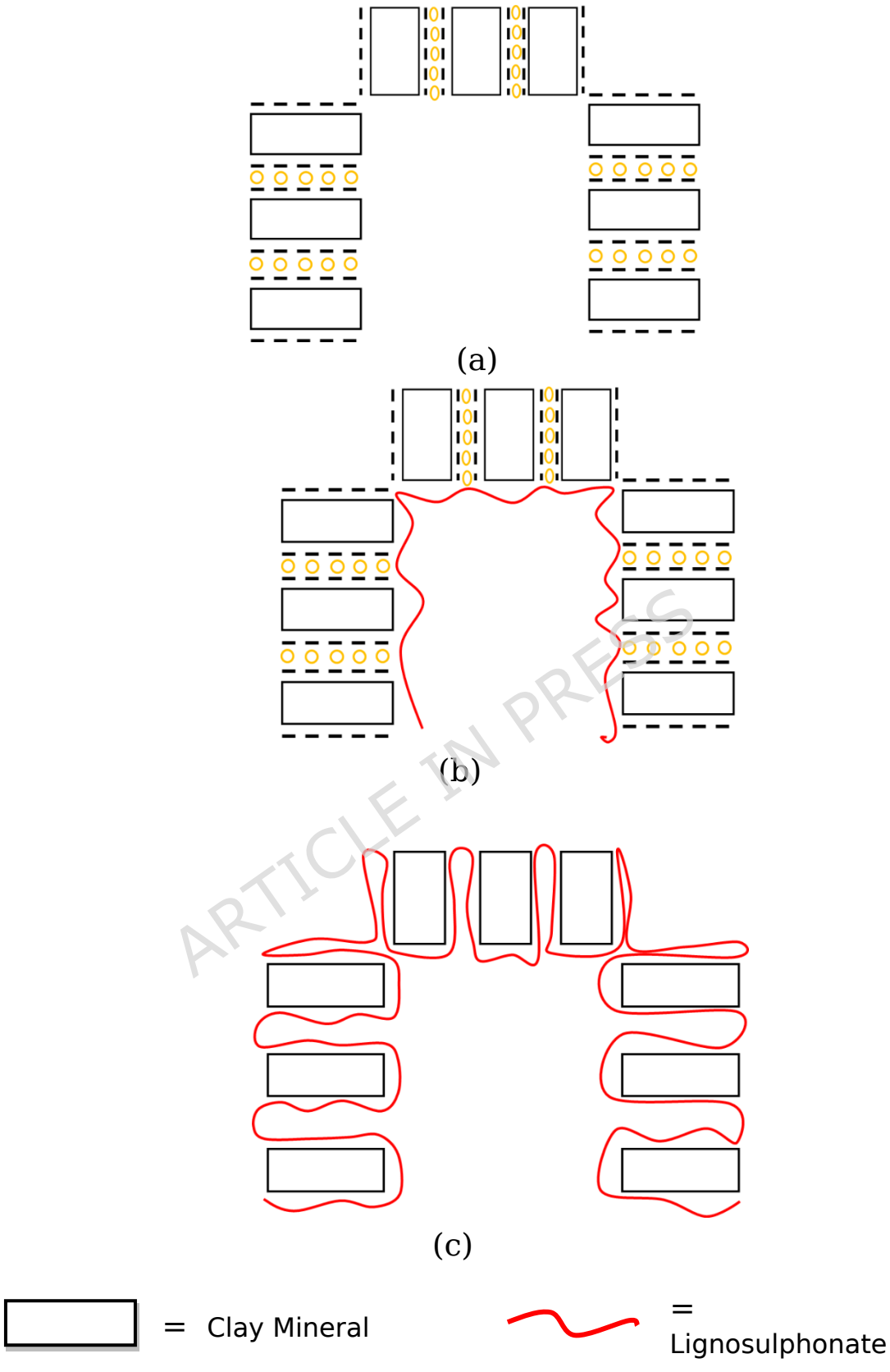

Fig. 17 Schematic diagram for lignin stabilized soil

4. Conclusion

The current study focuses on the behaviour of lignin-treated soil, specifically examining how varying lignin content affects the mechanical performance of stabilized soil mass and its swelling behaviour. Additionally, microstructural studies are conducted to understand the variations in the soil-lignin composites. Based on results presented, following conclusion can be drawn:

1. With increase in lignin content, both liquid limit (LL) and plasticity index (PI) decreased. However, beyond certain percentage of lignin (i.e., 0.75%) it again increases and becomes nearly constant indicating that the behavior of stabilized soil mass is highly sensitive to lignin additive.
2. Irrespective of percentage of lignin content, the unconfined compressive strength (UCS) found to be continuously increases with increase in curing period from *0* days to *28* days. For example, at lignin content of 0.75%, the UCS value found to be nearly same as virgin soil (i.e., 241 kPa) for 0 days of curing period whereas, it has been significantly increased to 362 kPa for curing period of 28 days. Hence, it can be said that the enhanced performance of stabilized soil is time dependent. Similar behavior has been observed through CBR (California Bearing Ratio) values as well.
3. The optimum sodium lignosulphonate content for the investigated low-plasticity clay (CL) was consistently found to be 0.75% by dry weight of soil, at which maximum UCS (362 kPa after 28 days), highest CBR, and minimum plasticity index and swell potential were achieved. Beyond this dosage, both strength and stiffness decrease progressively. This reduction is directly attributable to excess anionic lignosulphonate polymer chains that can no longer be adsorbed onto clay particle edges. The surplus negatively charged molecules increase inter-particle electrostatic repulsion and prevent the close particle-to-particle contact required for effective bonding. Macroscopically, this manifests as lower UCS and CBR values. Therefore, the optimum amount of lignin content can consider as

0.75% at which maximum performance of stabilized soil can be achieved.

4. Lignin addition significantly improves the soil's swelling capacity, as it reduces the swell potential to approximately by 20% of the virgin soil.
5. SEM micrographs demonstrate that the added material results in the formation of more stable aggregates and strong bonds between soil particles. Whereas, untreated clay reveals a flaky and discontinuous structure. In contrast, the SEM micrograph of treated clay shows that the electrostatic interactions transform the untreated granular structure into a more cohesive agglomerated mass, forming grain clusters.
6. Energy-dispersive X-ray spectroscopy (EDS) analysis revealed only minor variations in elemental ratios (e.g., Al:Si), indicating that sodium lignosulphonate primarily interacts physically with the clay rather than through significant new mineral formation. However, it should be noted that EDS is a semi-quantitative technique with known limitations for accurate mineralogical interpretation, including relatively high detection limits, influence of sample topography and coating, and overlap of characteristic X-ray peaks. Therefore, the observed small changes fall within typical measurement uncertainty and cannot be taken as conclusive evidence of chemical alteration.

5. Future Scope of the Study

The present study is limited to controlled laboratory conditions. Future research should therefore investigate the long-term field performance and durability of LS-stabilized low-plasticity clay under actual climatic variations and traffic loading. Large-scale field trials, such as test embankments or pavement sections, are recommended to verify the laboratory-observed strength gains and to assess constructability aspects not captured in small-scale specimens. In addition, the biodegradability of sodium lignosulphonate and its potential leaching behaviour in different

groundwater chemistries need to be evaluated to confirm its long-term environmental safety.

A particularly promising direction is the integration of artificial intelligence and machine learning for rapid, reliable prediction of LS-stabilized soil behaviour. Building on recent successful applications in cyclic soil response, can predict optimum LS dosage and long-term unconfined compressive strength from basic soil properties with significantly higher accuracy than conventional regression[57]. Similarly, deep-learning architectures such as long short-term memory (LSTM) networks, already proven effective for forecasting shear strain and excess pore-water pressure time histories in liquefiable sands[58], could be trained on the present UCS, CBR, and microstructural datasets to model time-dependent strength evolution and cyclic performance of LS-treated clay. Such data-driven and physics-informed hybrid models would substantially reduce the need for extensive trial-and-error experimentation, enable site-specific dosage optimization, and accelerate the adoption of this sustainable stabilizer in pavement subgrades and embankment construction worldwide.

Statement of originality

The authors declare that this manuscript is original, has not been published before and is not currently being considered for publication elsewhere. The authors confirm that the manuscript has been read and approved by all named authors and that no other persons have satisfied the criteria for authorship but are not listed. The authors further confirm that all have approved the order of authors listed in the manuscript of us. The authors understand that the corresponding author is the sole contact for the Editorial process. The corresponding author is responsible for communicating with the other authors about progress, submissions of revisions and final approval of proofs.

Additional information

No additional information is available for this paper.

Supplementary Materials

Not applicable.

Funding

This research received no external funding.

Institutional Review Board Statement

Not applicable.

Consent to Publish Declaration

Not applicable.

Clinical Trial Declarations

Not applicable.

Informed consent to participate

Not applicable.

Ethical Statement

This study did not involve human participants or animals; no ethical approval was required. All research procedures adhered to relevant ethical guidelines and best practices for non-human and non-animal research.

Data Availability Statement

Data used in the study is present in the manuscript.

Acknowledgements

The authors gratefully thank the authors' respective institutions for their strong support of this study.

Declaration of Interest statement

The authors declare no conflict of interest.

Declaration of AI use

The authors declare they will not use AI-assisted technologies to create this article.

Author Contribution

The authors have significantly contributed to this article's development and writing.

Credit authorship contribution statement

Ashutosh Kumar: Conceptualization, Data curation, Formal analysis, Investigation, Writing - original draft. **Prashant Kumar:** Project administration, Data curation, Formal analysis, Investigation, Writing – original draft, Writing – review and editing. **Awdhesh Kumar Choudhary:** Project administration, Data curation, Writing – original draft, Writing – review & editing. **Bamidele Charles Olaiya:** Writing – original draft, Writing – review and editing.

References:

1. Prusinski, J. R. & Bhattacharja, S. Effectiveness of Portland Cement and Lime in Stabilizing Clay Soils. Transp. Res. Rec. 1652, 215–227 (1999). doi:10.3141/1652-28

2. Saride, S., Puppala, A. & Chikyala, S. R. Swell-shrink and strength behaviors of lime and cement stabilized expansive organic clays. Appl. Clay Sci. 85, 39–45 (2013). doi:10.1016/j.clay.2013.09.008

3. Mohamad, N., Muthusamy, K., Embong, R., Kusbiantoro, A., & Hashim, M. H. Environmental impact of cement production and Solutions: A review. Materials Today: Proceedings, 48, 741-746 (2022). 48 , 741–746 (2022).

4. Chen, Q. & Indraratna, B. Shear behaviour of sandy silt treated with lignosulfonate. Can. Geotech. J. 52, 1180–1185 (2015).

5. Chew, S. H., Kamruzzaman, A. H. M. & Lee, F. H. Physicochemical and Engineering Behavior of Cement Treated Clays. J. Geotech. Geoenviron. Eng. 130, 696–706 (2004). doi:10.1061/(ASCE)1090-0241(2004)130:7(696)

6. Horpibulsuk, S., Miura, N. & Bergado, D. T. Undrained Shear Behavior of Cement Admixed Clay at High Water Content. J. Geotech. Geoenviron. Eng. 130, 1096–1105 (2004). doi:10.1061/(ASCE)1090-0241(2004)130:10(1096)

7. Horpibulsuk, S., Rachan, R. & Raksachon, Y. Role of Fly Ash on Strength and Microstructure Development in Blended Cement Stabilized Silty Clay. Soils Found. 49, 85–98 (2009). doi:10.3208/sandf.49.85

8. Chen, Q., Indraratna, B., Carter, J. & Rujikiatkamjorn, C. A theoretical and experimental study on the behaviour of lignosulfonate-treated sandy silt. Comput. Geotech. 61, 316–327 (2014). doi:10.1016/j.compgeo.2014.06.010

9. Latifi, N., Eisazadeh, A., Marto, A. & Meehan, C. L. Tropical residual soil stabilization: A powder form material for increasing soil strength. Constr. Build. Mater. 147, 827–836 (2017). doi:10.1016/j.conbuildmat.2017.04.115

10. Zhang, T., Cai, G. & Liu, S. Application of Lignin-Stabilized Silty Soil in Highway Subgrade: A Macroscale Laboratory Study. J. Mater. Civ.

Eng. 30, 04018028 (2018). doi:10.1061/(ASCE)MT.1943-5533.0002203

11. Bayesteh, H. & Hezareh, H. Behavior of cement-stabilized marine clay and pure clay minerals exposed to high salinity grout. Constr. Build. Mater. 383, 131334 (2023). doi:10.1016/j.conbuildmat.2023.131334

12. Rao, S. & Thyagaraj, T. Lime slurry stabilisation of an expansive soil. Proc. Inst. Civ. Eng. Geotech. Eng. 156, 139–146 (2003). doi:10.1680/geng.156.3.139.37296

13. Chen, Q. & Indraratna, B. Deformation Behavior of Lignosulfonate-Treated Sandy Silt under Cyclic Loading. J. Geotech. Geoenviron. Eng. 141, 04014091 (2015). doi:10.1061/(ASCE)GT.1943-5606.0001210

14. Alazigha, D. P., Indraratna, B., Vinod, J. S. & Ezeajugh, L. E. The swelling behaviour of lignosulfonate-treated expansive soil. Proc. Inst. Civ. Eng. Ground Improv. 169, 99–112 (2016). https://ro.uow.edu.au/eispapers/5802

15. Ta'negonbadi, B. & Noorzad, R. Stabilization of clayey soil using lignosulfonate. Transp. Geotech. 12, 45–55 (2017). doi:10.1016/j.trgeo.2017.08.004

16. Sagastume Gutiérrez, A., Van Caneghem, J., Cogollos Martínez, J. B. & Vandecasteele, C. Evaluation of the environmental performance of lime production in Cuba. J. Clean. Prod. 31, 126–136 (2012). doi:10.1016/j.jclepro.2012.02.035

17. Tingle, J. S., Newman, J. K., Larson, S. L., Weiss, C. A. & Rushing, J. F. Stabilization Mechanisms of Nontraditional Additives. Transp. Res. Rec. 1989, 59–67 (2007). doi:10.3141/1989-49

18. Arulrajah, A., Mohammadinia, A., Maghool, F. & Horpibulsuk, S. Tire derived aggregates as a supplementary material with recycled

demolition concrete for pavement applications. J. Clean. Prod. 230, 129–136 (2019). doi:10.1016/j.jclepro.2019.05.084

19. Latifi, N., Vahedifard, F., Ghazanfari, E. & Rashid, A. S. A. Sustainable Usage of Calcium Carbide Residue for Stabilization of Clays. J. Mater. Civ. Eng. 30, 04018194 (2018). doi:10.1061/(ASCE)MT.1943-5533.0002313

20. Vijayan, G. & Sasikumar, A. Stabilisation of Clayey Soil by using Lignosulfonate. Int. Res. J. Eng. Technol. (2008).

21. Vinod, J. S., Indraratna, B. & Al Mahamud, M. A. Stabilisation of an erodible soil using a chemical admixture. Proc. Inst. Civ. Eng. Ground Improv. 163, 43–51 (2010). doi:10.1680/grim.2010.163.1.43

22. Indraratna, B., Athukorala, R. & Vinod, J. Estimating the Rate of Erosion of a Silty Sand Treated with Lignosulfonate. J. Geotech. Geoenviron. Eng. 139, 701–714 (2013). doi:10.1061/(ASCE)GT.1943-5606.0000766

23. Yang, B. et al. Assessment of soils stabilized with lignin-based byproducts. Transp. Geotech. 17, 122–132 (2018). doi:10.1016/j.trgeo.2018.10.005

24. Ijaz, N., Dai, F., Meng, L., Rehman, Z. ur & Zhang, H. Integrating lignosulphonate and hydrated lime for the amelioration of expansive soil: A sustainable waste solution. J. Clean. Prod. 254, 119985 (2020). doi:10.1016/j.jclepro.2020.119985

25. Gopalakrishnan, K., Ceylan, H. & Kim, S. Renewable biomass-derived lignin in transportation infrastructure strengthening applications. Int. J. Sustain. Eng. 6, 316–325 (2013). doi:10.1080/19397038.2012.730069

26. Zhang, T., Cai, G. & Liu, S. Application of lignin-based by-product stabilized silty soil in highway subgrade: A field investigation. J.

Clean. Prod. 142, 4243–4257 (2017). doi:10.1016/j.jclepro.2016.12.002

27. Zhang, T., Cai, G. & Liu, S. Reclaimed Lignin-Stabilized Silty Soil: Undrained Shear Strength, Atterberg Limits, and Microstructure Characteristics. J. Mater. Civ. Eng. 30, 04018270 (2018). doi:10.1061/(ASCE)MT.1943-5533.0002492

28. Ta'negonbadi, B. & Noorzad, R. Physical and geotechnical long-term properties of lignosulfonate-stabilized clay: An experimental investigation. Transp. Geotech. 17, 41–50 (2018). doi:10.1016/j.trgeo.2018.09.001

29. Alazigha, D. P., Indraratna, B., Vinod, J. S. & Heitor, A. Mechanisms of stabilization of expansive soil with lignosulfonate admixture. Transp. Geotech. 14, 81–92 (2018). doi:10.1016/j.trgeo.2017.11.001

30. Zhang, T., Liu, S., Zhan, H., Ma, C. & Cai, G. Durability of silty soil stabilized with recycled lignin for sustainable engineering materials. J. Clean. Prod. 248, 119293 (2020). doi:10.1016/j.jclepro.2019.119293

31. Santoni, R. L., Tingle, J. S. & Webster, S. L. Stabilization of Silty Sand with Nontraditional Additives. Transp. Res. Rec. 1787, 61–70 (2002). doi:10.3141/1787-07

32. Olaiya, B.C., Lawan, M.M. & Olonade, K.A. Utilization of sawdust composites in construction—a review. SN Appl. Sci. 5, 140 (2023). https://doi.org/10.1007/s42452-023-05361-4

33. Olaiya, B.C., Lawan, M.M., Olonade, K.A. et al. An overview of the use and process for enhancing the pozzolanic performance of industrial and agricultural wastes in concrete. Discov Appl Sci 7, 164 (2025). https://doi.org/10.1007/s42452-025-06586-1

34. Ceylan, H., Gopalakrishnan, K. & Kim, S. Soil stabilization with bioenergy coproduct. Transp. Res. Rec. 2186, 130–137 (2010). doi:10.3141/2186-14

35. Sharmila, B., Bhuvaneshwari, S. & Landlin, G. Application of lignosulphonate—a sustainable approach towards strength improvement and swell management of expansive soils. Bull. Eng. Geol. Environ. 80, 6395–6413 (2021). doi:10.1007/s10064-021-02323-1

36. Olaiya, B.C., Lawan, M.M., Olonade, K.A. et al. Banana leaf ash as sustainable alternative raw material for the production of concrete: a review. Discov Mater 5, 100 (2025). https://doi.org/10.1007/s43939-025-00296-6

37. Shulga, G. et al. New lignin-based polymers for ecological rehabilitation. Mol. Cryst. Liq. Cryst. 486, 291–305 (2008). doi:10.1080/15421400801921926

38. Kumar, Padam Siva, Pramod Kumar, N. Manikandan, P. Thejasree, Neeraj Sunheriya, Jayant Giri, Rajkumar Chadge, T. Sathish, Ajay Kumar, and Muhammad Imam Ammarullah. "A sustainable bioengineering approach for enhancing black cotton soil stability using waste foundry sand." International Journal of Low-Carbon Technologies 20 (2025): 1112-1120.

39. Liu, Y. et al. Use of Sulfur-Free Lignin as a novel soil additive: A multi-scale experimental investigation. Eng. Geol. 269, 105551 (2020). doi:10.1016/j.enggeo.2020.105551

40. Wu, D. et al. Stabilization Mechanism of Calcium Lignosulphonate Used in Expansion Sensitive Soil. J. Wuhan Univ. Technol. Mater. Sci. Ed. 35, 847–855 (2020). doi:10.1007/s11595-020-2329-y

41. Zhang, T., Yang, Y. L. & Liu, S. Y. Application of biomass by-product lignin stabilized soils as sustainable Geomaterials: A review. Sci.

Total Environ. 728, 138830 (2020). doi:10.1016/j.scitotenv.2020.138830

42. Sarker, D., Shahrear Apu, O., Kumar, N., Wang, J. X. & Lynam, J. G. Application of Sustainable Lignin Stabilized Expansive Soils in Highway Subgrade. in Geo-Congress 2021 336–348 (American Society of Civil Engineers, 2021). doi:10.1061/9780784483435.033

43. Vakili, A. H., Kaedi, M., Mokhberi, M., Selamat, M. & Salimi, M. Treatment of highly dispersive clay by lignosulfonate addition and electroosmosis application. Appl. Clay Sci. 152, 1–8 (2018). doi:10.1016/j.clay.2017.11.039

44. Olaiya, B.C., Lawan, M.M., Olonade, K.A. et al. Development of sustainable sandcrete bricks using industrial and agricultural waste. Sci Rep 15, 17202 (2025). https://doi.org/10.1038/s41598-025-02308-0

45. Olaiya, B.C., Aliyu, S., Obeagu, E.I. et al. Sustainable building practices for modern clinical laboratories. Discov Civ Eng 2, 74 (2025). https://doi.org/10.1007/s44290-025-00232-w

46. Charles Olaiya, B., George Fadugba, O., & Muhammad Lawan, M. (2024). Building Information Modeling (BIM) Implementation and Practices in Construction Industry: A Review. IntechOpen. doi: 10.5772/intechopen.1006363

47. ASTM International. ASTM D6913/D6913M-17 Standard Test Methods for Particle-Size Distribution (Gradation) of Soils Using Sieve Analysis. (ASTM International, 2009). doi:10.1520/D6913_D6913M-17

48. ASTM International. ASTM D4318-10 Standard Test Methods for Liquid Limit, Plastic Limit, and Plasticity Index of Soils. (ASTM International, 2010).

49. ASTM International. ASTM D2487-11 Standard Practice for Classification of Soils for Engineering Purposes (Unified Soil Classification System). (ASTM International, 2011).

50. ASTM International. ASTM D698-07 Standard Test Methods for Laboratory Compaction Characteristics of Soil Using Standard Effort. (ASTM International, 2007).

51. ASTM International. ASTM D4972-13 Standard Test Method for pH of Soils. (ASTM International, 2013).

52. ASTM International. ASTM D854-14 Standard Test Methods for Specific Gravity of Soil Solids by Water Pycnometer. (ASTM International, 2014).

53. ASTM International. ASTM D2166-13 Standard Test Method for Unconfined Compressive Strength of Cohesive Soil. (ASTM International, 2013).

54. ASTM International. ASTM D4219-08 Standard Test Method for Unconfined Compressive Strength Index of Chemical-Grouted Soils. (ASTM International, 2008).

55. ASTM International. ASTM D1883-14 Standard Test Method for California Bearing Ratio (CBR) of Laboratory-Compacted Soils. (ASTM International, 2014).

56. ASTM International. ASTM D4546-08 Standard Test Methods for One-Dimensional Swell or Collapse Potential of Cohesive Soils. (ASTM International, 2008).

57. Jas, K., Jana, A. & Dodagoudar, G. R. Evaluation and Future Prospects of Data-Driven Intelligence-Based Framework for Predicting Cyclic Behavior of Reconstituted Sand. Int. J. Numer. Anal. Methods Geomech. 49, 1597–1621 (2025). doi:10.1002/nag.3939

58. Jas, K. & Jana, A. Prediction of shear strain and excess pore water pressure response in liquefiable sands under cyclic loading using

deep learning model. Jpn. Geotech. Soc. Spec. Publ. 10, 1729–1734 (2024). doi:10.3208/jgssp.v10.OS-35-05